Available online at www.sciencedirect.com

ScienceDirect

Procedia Structural Integrity 11 (2018) 161–168

Structural Integrity Procedia

www.elsevier.com/locate/procedia

XIV International Conference on Building Pathology and Constructions Repair – CINPAR 2018

Verification of an energy-based design procedure for seismic retrofit of a school building

Gloria Terenzi[a,]*, Iacopo Costoli[a], Stefano Sorace[b], Paolo Spinelli[a]

[a]*Department of Civil and Environmental Engineering, University of Florence, Via S. Marta 3, 50139Florence, Italy*
[b]*Polytechnic Department of Engineering and Architecture, University of Udine, Via delle Scienze 206, 33100 Udine, Italy*

Abstract

A viable design criterion of supplemental damping strategies for seismic retrofit of frame structures, recently proposed by the first author (Terenzi, 2018), is applied in this paper to a school building in Florence dating back to the early 1980s. The building is composed of two portions, with reinforced concrete and steel frame structure, respectively. Similarly to several other buildings of the same period, the structure is infilled by heavy reinforced concrete panels interacting with the frame elements under horizontal loads. A careful reconstruction of the structural characteristics of the constituting members, based on the original design documentation and on-site testing campaigns, highlighted specific drawbacks in current state, related to a remarkable degration of the materials and a poor performance of several elements. The retrofit solution considered in this study consists in removing the infill panels and replacing them with a set of dissipative braces incorporating fluid viscous dampers as protective devices. The design is carried out by the sizing criterion mentioned above, targeting an elastic structural response up to the maximum considered earthquake normative level.

Keywords: Seismic retrofit; supplemental damping; energy-based design procedures; school buildings.

1. Introduction

The high vulnerability of the Italian built heritage, highlighted once again by the earthquakes that hit Marche, Umbria and Lazio regions beginning from August 2016, is increasingly motivating local authorities to promote

* Corresponding author: Gloria Terenzi. Phone: +39.055.2758887; fax: +39.055.2758000.
E-mail address: gloria.terenzi@unifi.it

10.1016/j.prostr.2018.11.022

seismic performance assessment campaigns of public buildings, including schools. The study proposed in this paper, concerning a school built in Florence in the 1980s, belongs to this line of activity.

The building is characterized by geometric irregularities in elevation, and the structure is constituted by reinforced concrete (R/C) walls on the basement, and reticular steel beams and columns on the ground and first story. On-site tests revealed an unsatisfactory state of conservation of the welds of the latter. A detailed seismic assessment analysis carried out in current conditions highlighted also significant deficiencies of several columns in terms of shear and axial force strength, as well as possible instability conditions of the constituting profiles. These problems are increased by the presence of large precast cladding panels, which produce severe loading conditions on these members.

Based on the performance conditions of the structure in current state, local interventions in the steel beams with damaged welds and the replacement of the external panels with lighter ones, are proposed to reach safe conditions under gravity loads. Furthermore, a retrofit solution consisting in the installation of a dissipative bracing system incorporating silicone fluid-viscous (FV) devices is designed, aimed at significantly improving the seismic performance of the building too.

2. Case study school building

The school building has a rectangular plan, with maximum external dimensions of (31×38.7) m×m. The average floor area is about 1070 m^2 and the total volume is 10950 m^3. The storey heights are equal to 3.3 m (basement storey) and 3.75 m (remaining storeys). The first floor is accessed through two internal flights of stairs, one of which connects it with the ground floor only, and the other one with all storeys. In addition, three external staircases connect the basement with the main entrance floor. A structural joint separates the building from a more recent elevator compartment made of a 250 mm-thick R/C box section. The roof is flat. Figure 1 shows the ground floor plan including the numbering of beams (1 and 2, whereas number 3 is referred to the alignments of the R/C basement walls), whose sections are detailed in Figures 2 and 3.

Due to a lack of original design documentation, an extensive on-site testing campaign was preliminarily carried out. Pacometric tests allowed identifying the reinforcement of the R/C beams, columns and walls. As a result, Φ16 longitudinal bars and 250 mm-spaced Φ8 stirrups were located in beams, with cross sections of (280×920) mm×mm (number 1 in Figure 1) and (400×920) mm×mm (number 2). The columns are of two types too, with dimensions of (420×420) mm×mm (corner alignments — A5, B6, F6, A3, B2 and F2 in Figure 1) and (400×400) mm×mm (remaining alignments), reinforced with Φ16 bars and 200-through-250 mm spaced Φ8 stirrups. The floors are in reinforced concrete, of “Predalles” type on the ground and first floor, and made of prefabricated joists and clay bricks, on the roof.

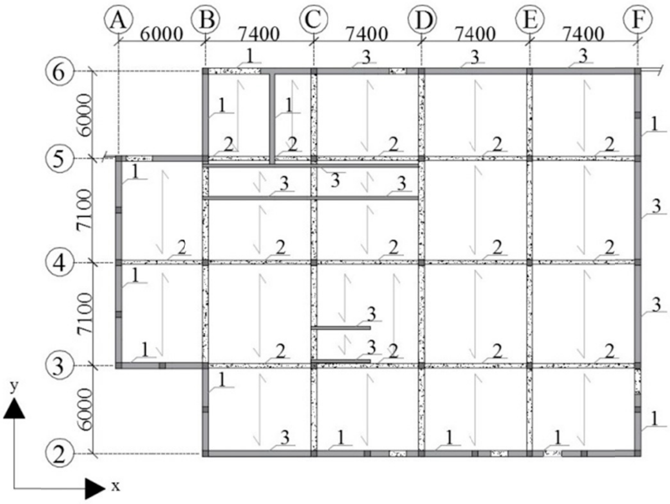

Fig. 1. Ground floor plan with alphanumerical alignment identification and R/C beam numbering.

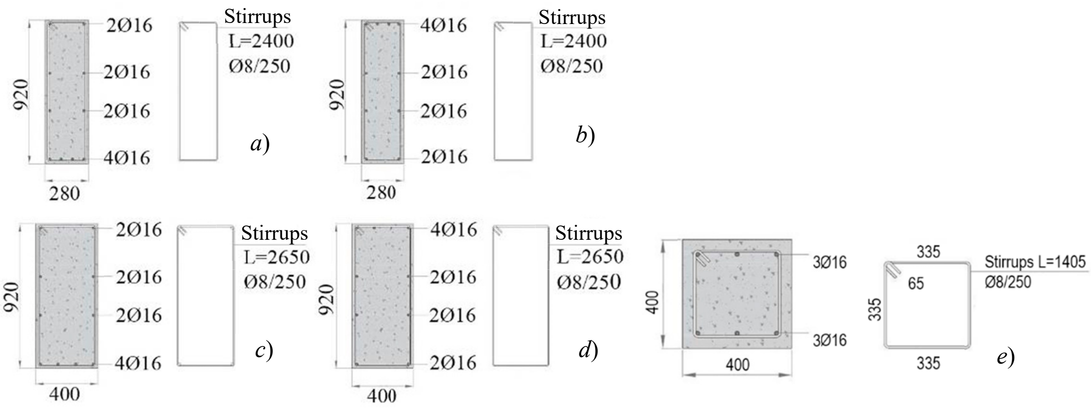

Fig. 2. Type 1 (*a-b*) and type 2 (*c-d*) beam sections at half-span (*a-c*) and the ends (*b-d*); column section in the basement storey (*e*).

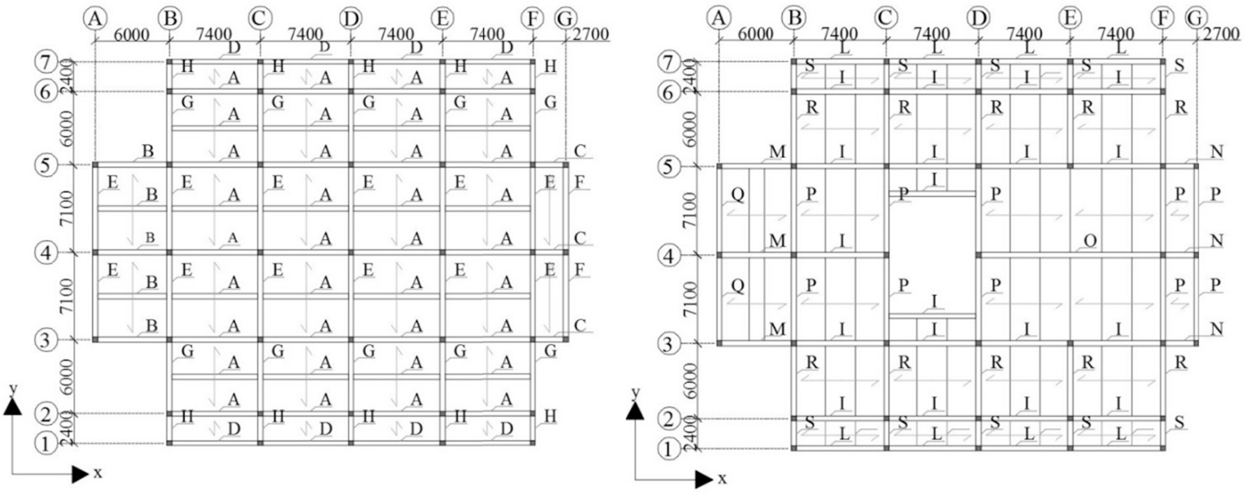

Fig. 3. First floor (*a*) and roof (*b*) plans with alphanumerical alignment identification and steel beam lettering.

The reticular steel members of the ground and first storey include 17 different types of beams, as indicated in the plans in Figure 3 and displayed in Figure 4, and a single type of columns, shown in Figure 5.

The on-site testing programme consisted in: 3 core drillings in the basement, 18 pacometric surveys and a reinforcement sample in the ground and first storey, for the R/C members; 6 microdurometer and electric resistance tests on the welds of 12 steel joints, and several magnetoscopic tests, for the steel elements. Based on the prescriptions of the Italian Technical Standards (Italian Council of Public Works 2008, 2009)., the tests allowed meeting the "basic knowledge" level (named LC1) for the structural assessment analysis of public buildings. The corresponding value of the "confidence factor", i.e. the additional knowledge level-related safety coefficient to be introduced in stress state checks, is equal to 1.35.

The following main properties resulted from the characterization tests: mean cubic compressive strength of concrete equal to 24 N/mm^2; yield stress and tensile strength of steel equal to 324 MPa and 462 MPa, respectively; yield stress of the steel members equal to 204 MPa.

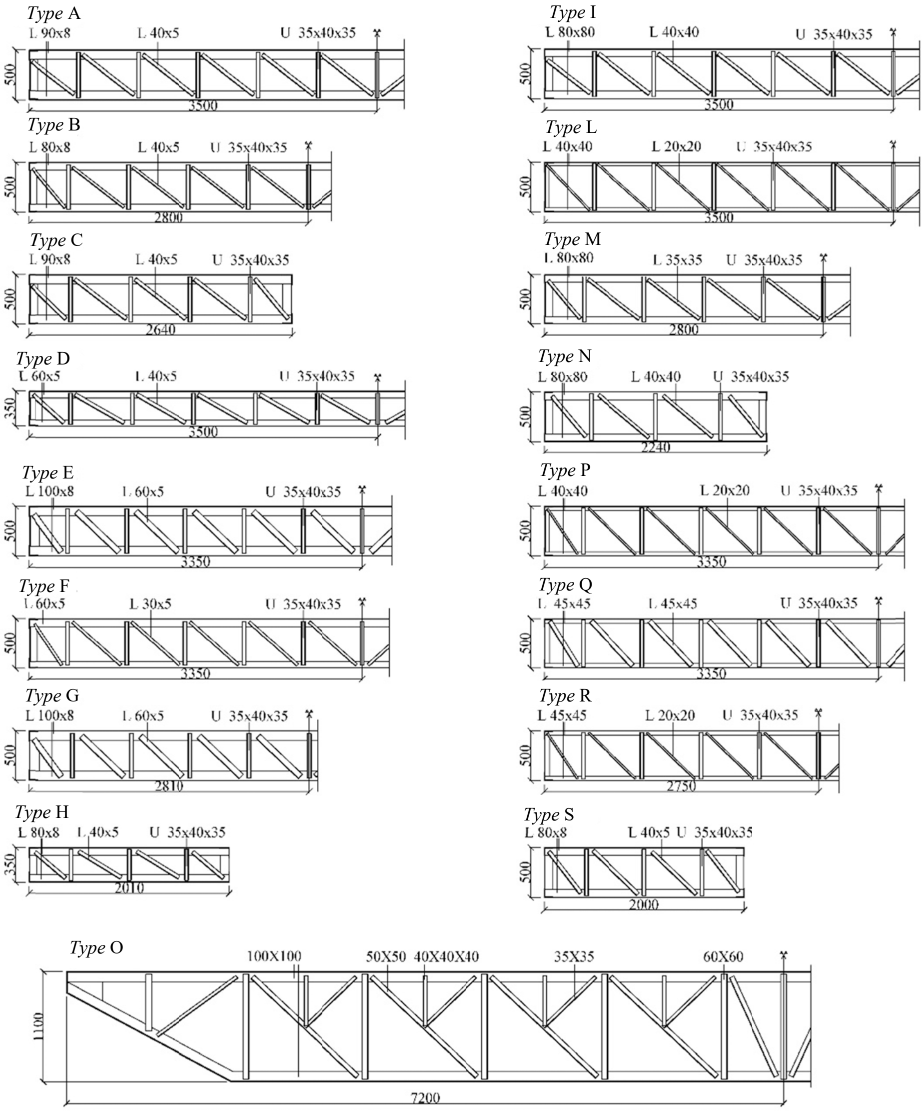

Fig. 4.Ground and first storey reticular steel beams (types A through S).

3. Assessment analysis in current conditions

The verification enquiry in current conditions is articulated in a modal analysis, to calculate the vibration periods and associated modal masses, and a time-history analysis, to assess the seismic performance in terms of stress states and displacements.

3.1. Modal analysis

The finite element model of the structure was generated by SAP2000NL calculus program (CSI, 2018), using frame type elements for all members. The cladding panels were considered as equivalent concentrated loads at the ends of the steel beams. To take into account the poor strength of the welds of the steel beams and columns highlighted by the investigation campaign, rotational releases were inserted at the ends the constituting trusses.

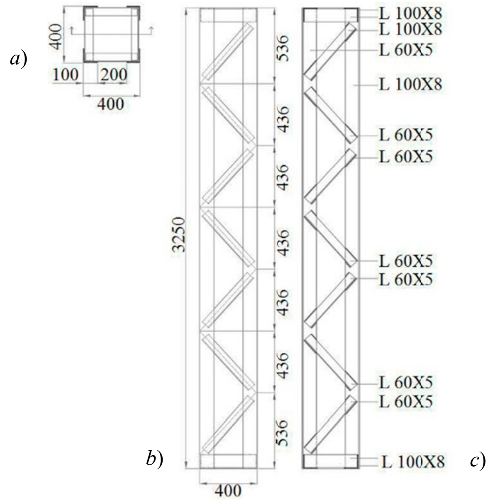

Fig. 5. Steel columns on the ground and the first storey; section (*a*), lateral view (*b*) and constituting profiles (*c*).

The modal analysis showed two first horizontal translational modes along *X* and *Y*, with nearly coinciding vibration periods of 0.466 s (*Y*) and 0.46 s (*X*), respectively, and effective modal masses (EMMs) equal to 46.5% along *Y*, and 38.9% along *X*. The above-mentioned structural irregularity in height gives rise to not negligible modal contributions up to the thirteenth mode, by which summed modal masses greater than 85% are activated in both directions (equal to 88.7% along *X*, and 85.3% along *Y*).

3.2. Time-history verification and performance assessment analysis

The performance evaluation enquiry was carried out for the four reference seismic levels fixed in the Italian Standards (Italian Public Works 2008), that is, Frequent Design Earthquake (FDE, with 81% probability of being exceeded over the reference time period V_R); Serviceability Design Earthquake (SDE, with 50%/V_R probability); Basic Design Earthquake (BDE, with 10%/V_R probability); and Maximum Considered Earthquake (MCE, with 5%/V_R probability). The V_R period is fixed at 75 years, which is obtained by multiplying the nominal structural life V_N of 50 years by a coefficient of use C_u equal to 1.5, imposed to school buildings. By referring to topographic category T1 (flat surface), and B-type soil, the resulting peak ground accelerations for the four seismic levels referred to the city of Florence are as follows: 0.065 *g* (FDE), 0.078 *g* (SDE), 0.181 *g* (BDE), and 0.227 *g* (MCE).

The results of the analysis carried out in current state are synthesized, in terms of displacement response, in Figure 6, where the interstorey drifts normalized to the storey heights are plotted for *X* (d_{ix} – Figure 6*a*) and *Y* (d_{iy} – Figure 6*b*) directions. As shown by these diagrams, all values calculated for the SDE-scaled seismic action are below the Immediate Occupancy level threshold ($d_{i,IO}$=0,5%). At the same time, they only slightly exceed the Operational performance level limitation ($d_{i,OP}$=0,33%) on the second storey, where the normalized drift reaches 0,35%. At the BDE and MCE seismic levels the drifts are neatly below the 2% threshold suggested for steel structures at the Life Safety performance level by the American Standard ASCE-41.

On the other hand, the axial force instability limits computed for the vertical profiles of columns (L profiles with dimensions of 100×8 mm×mm), as well as the diagonal ones (L profiles 60×5 mm×mm), respectively equal to 298.2 kN and 85.1 kN, are exceeded by a factor equal to about 1.5, at the BDE, and about 2, at the MCE. Similar deficiencies were found also in the cantilever beams supporting the cladding panels.

4. Retrofit hypothesis

Based on the results of the assessment analysis in current conditions, a retrofit solution aimed at improving the seismic performance of the steel members both locally, by strengthening the steel cantilever beams, and globally, by introducing a dissipative bracing system in both directions in plan, was proposed. The intervention on the cantilever beams consists in welding shaped plates on the diagonal profiles over their entire length, in order to protect the damaged welds from the risk of collapse. The global seismic retrofit strategy is represented by the installation of the system in 16 vertical alignments, all adjacent to the building corners. The incorporated FV devices were designed according to the criterion discussed in the following sections.

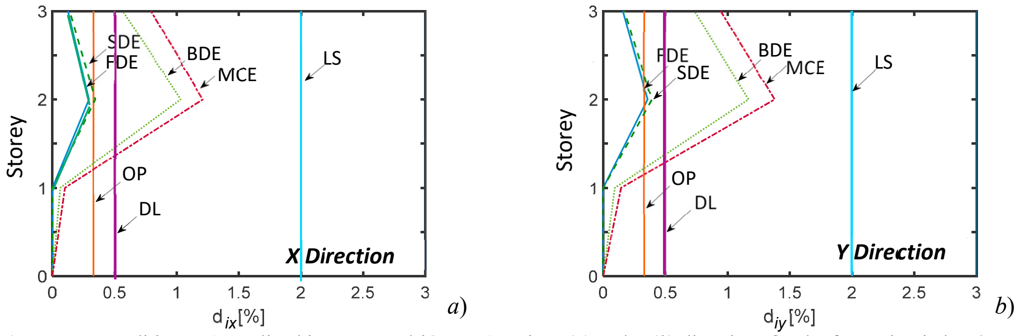

Fig. 6. Current conditions. Normalized interstorey drift envelops in *X* (*a*) and *Y* (*b*) directions for the four seismic levels.

4.1. Mechanical characteristics of FV devices

The dissipative braces were incorporated in the B2-B3, B2-C2, B5-B6, B6-C6, E2-F2, E6-F6, F2-F3, F5-F6 bays (Figure 3), on the ground storey, and the B1-C1, B2-B3, B5-B6, B7-C7, E1-F1, E7-F7, F5-F6, F2-F3 bays, on the first storey. A view of the finite element model including the seismic protection system is shown in Figure 7. The FV dampers are installed in pairs at the tip of the supporting diagonal trusses, with inverted V-shaped layout, as illustrated by the drawings in the same Figure.

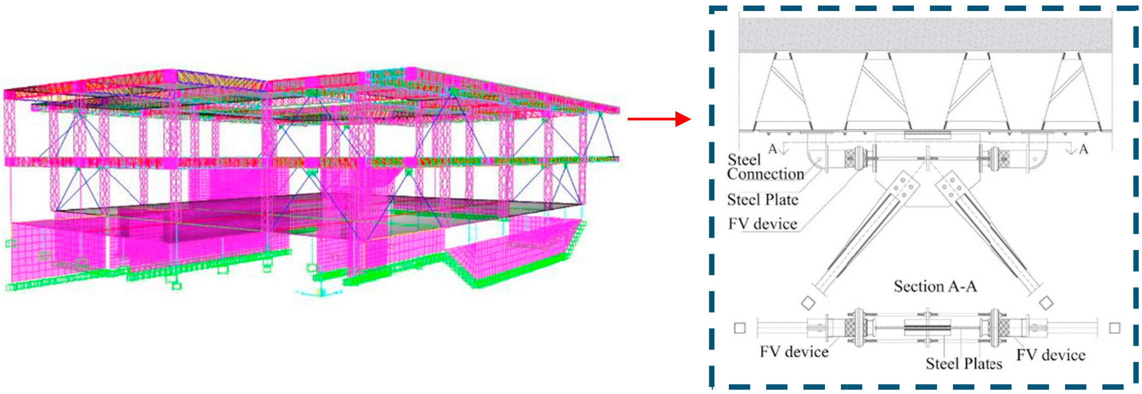

Fig. 7. Finite element model of the building incorporating the dissipative bracing system and installation details.

Differently from other classes of dampers, FV devices provide a very high dissipative action with small stiffening effects, which represents an effective property for rather stiff structures, like the case study one. The mechanical behaviour of FV devices is characterized by the following damping and elastic response force components (Terenzi 1999; Sorace and Terenzi 2001):

$$F_d = c \cdot sgn[\dot{x}(t)]|\dot{x}(t)|^{\alpha} \tag{1}$$

$$F_{ne}(t) = k_2 x(t) + \frac{(k_1 - k_2)\,x(t)}{\left[1 + \left|\frac{k_1 x(t)}{F_0}\right|^5\right]^{1/5}} \tag{2}$$

where: t = time variable; c = damping coefficient; sgn(·) = signum function; $\dot{x}(t)$ = velocity; |·| absolute value: α = fractional exponent, ranging from 0.1 to 0.2 (Sorace and Terenzi 2001); F_0 = static pre-load; k_1, k_2 = stiffness of the response branches situated below and beyond F_0; $x(t)$ = displacement.

4.2. Sizing design procedure of the FV dampers and performance verification in retrofitted conditions

The design procedure applied for preliminarily sizing the FV devices is based on the assumption that, as observed above, for relatively stiff frame structures a substantial improvement of seismic performance can be reached by incorporating a supplemental damping system with limited stiffening capacity. For more deformable structures, a supplemental stiffness contribution helps control lateral displacements better, prevents over-dissipation demands to the protective technology adopted (Sorace et al. 2016, Terenzi 2018). The FV dampers were designed based on the sizing procedure proposed in Terenzi (2018), by referring to its implementation for structures with poor shear and/or bending moment strength of constituting members. The procedure starts by assuming prefixed reduction factors, α_s, of the most critical response parameters in current conditions, which are evaluated by means of a conventional elastic finite element analysis. Simple formulas relating the reduction factors to the equivalent viscous damping ratio of the dampers, ξ_{eq}, allow calculating the ξ_{eq} values that guarantee the achievement of the target reduction factors. Finally, the energy dissipation capacity of the devices is deduced from ξ_{eq}, finalizing their sizing process.

The application of this procedure to the case study school building is aimed at checking the effectiveness of the method also in the special case of steel structures with instability problems in the constituting members. Furthermore, as the columns are of reticular type, the α_s calculation must be related to the axial force in the vertical trusses. Therefore, said N_{tj}^a the maximum axial force evaluated in current condition for the most stressed truss constituting the columns in the j-th interstorey, and N^{cr} the corresponding critical force value, the corresponding α_s ratio is given by:

$$\alpha_s = \frac{N_{tj}^a}{N^{cr}} \tag{3}$$

By introducing this relation in the ξ_{eq} equation (Terenzi 2018):

$$\xi_{eq} = \frac{2(\alpha_s - 1)}{\pi\alpha_s} \tag{4}$$

and substituting ξ_{eq} in the dissipated energy expression

$$E_D = 2\pi\alpha_s F_e \xi_{eq} d_{d,max} \tag{5}$$

where: F_e = elastic base shear of the structure, and $d_{d,max}$ = maximum displacement of the devices, it can be estimated the energy dissipation capacity of the dampers, E_D, and then selected the devices with the nearest mechanical characteristics, as identified from the manufacturer's catalogue (Jarret 2018).

The verification analysis in current conditions highlights the most critical axial force in the corner columns B-1, F-1, B-7, F-7, in both storeys and for both directions. For the MCE-scaled seismic action N_{tj}^a reaches 653 kN (first storey) and 450 kN (second storey) in the F-7 column. Thus, the corresponding stress reduction factors α_s are as follows: α_{s1} = 2.19; α_{s2} = 1.5. Based on these values, the equivalent viscous damping ratios of the set of FV dampers to be installed on the two levels, calculated by means of relation (4), are: $\xi_{eq,1}$ = 0.345; $\xi_{eq,2}$ = 0.21.

Then, the E_D energy dissipation capacity of the spring–dampers is calculated by (5), assuming the following values of the elastic limit shear of the j-th level in X, $F_{ej,X}$, and Y, $F_{ej,Y}$ (i.e., the sum of the elastic limit shear forces of the columns in the j-th storey), and the corresponding maximum drifts $d_{dj,max,X}$, $d_{dj,max,Y}$: $F_{e1,X} = F_{e1,Y}$ = 4076 kN; $F_{e2,X} = F_{e2,Y}$ = 114.3 kN; $d_{d1,max,X}$ = 27.1 mm; $d_{d1,max,Y}$ = 28.4 mm; $d_{d2,max,X}$ = 10.3 mm; $d_{d2,max,Y}$ = 12.8 mm. Introducing these values, as well as the above-mentioned α_{sj} and $\xi_{eq,j}$ values, in (5), the following E_D estimate is derived for each direction and level: $E_{D1,X}$ = 524 kJ; $E_{D1,Y}$ = 549 kJ; $E_{D2,X}$ = 2.3 kJ; $E_{D2,Y}$ = 2.9 kJ. The extreme difference in the dissipation demand for the two storeys depends on relevant seismic masses, equal to 831 kN/g (first storey – m_1), and 233 kN/g (second storey – m_2), respectively, as a consequence of the significantly different distribution of the cladding panels. The design of the dampers was finally based on the total dissipated energy in the two directions: $E_{Dtot,X}$ = 526 kJ; $E_{Dtot,Y}$ = 552 kJ. By dividing these values by the number of spring–dampers placed in X and Y, the maximum energy dissipation capacity $E_{D,X,dmax}$ ($E_{D,Y,dmax}$) that could be assigned to each of the sixteen devices in order to reach the target performance at the MCE results as follows: $E_{D,X,dmax}$ = 32.9 kJ ($E_{D,Y,dmax}$ = 34.5 kJ). By considering these upper sizing limit, in order to reasonably constrain the dimensions of the devices and the cost of the intervention, as a first retrofit hypothesis it was assumed the most performing device model belonging to the smallest series in standard manufacturing, with the following mechanical characteristics: E_n = 14 kJ (i.e. about half the upper sizing limit); stroke s_{max} = ±40 mm; damping coefficient c = 14.16 kN(s/mm)$^{\gamma}$, with γ = 0.15; F_0 = 28 kN; and k_2 = 2.1 kN/mm.

Based on this assumption, the seismic performance in retrofitted conditions was evaluated, which showed the normalized drift profiles graphed in Figure 8. A satisfactory response is observed, as the drifts do not exceed the IO-related limit, in both directions, up to the MCE earthquake level. On the other hand, in terms of stress states, the axial forces in the vertical profiles of the first storey columns — although remarkably reduced — are approximately 40% higher than relevant critical values. This is a consequence of the reduced damping capacity of the dissipaters assumed, aimed at constraining the intervention costs.

Further developments of the study will concern the adoption of FV devices with greater sizes, so as to finally provide a comprehensive cost/benefit analysis for the seismic retrofit of case study building.

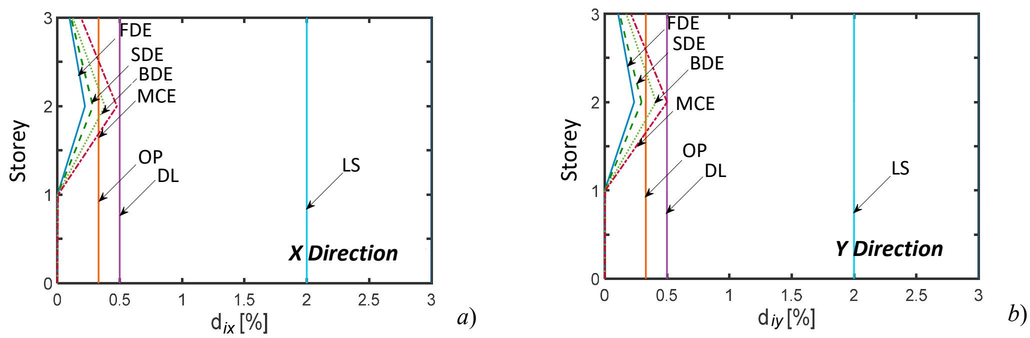

Fig. 8. Retrofitted conditions. Normalized inter-storey drift envelops in X (a) and Y (b) directions for the four seismic levels.

Acknowledgments

The study reported in this paper was sponsored by the Italian Department of Civil Protection within the ReLUIS-DPC Project 2014/2018, Research Line 6: Isolation and Dissipation. The author gratefully acknowledge this financial support.

References

ASCE/SEI 41-06, 2006. Seismic Rehabilitation of Existing Buildings, American Society of Civil Engineers: Reston, VA, USA.

ASCE 7-10, 2010. Minimum Design Loads for Buildings and Other Structures, American Society of Civil Engineers: Reston, VA, USA.

Italian Council of Public Works, 2008. Technical Standards on Constructions, Italian Council of Public Works: Rome, Italy.

Italian Council of Public Works, 2009. Commentary on the Technical Standards on Constructions, Italian Council of Public Works: Rome, Italy.

Jarret, S.L., 2018. Shock-Control Technologies. Available online: http://www.introini.info.

SAP2000NL, 2018. Theoretical and Users' Manual, Release 18.05. Computers & Structures Inc.: Berkeley, CA, USA.

Sorace, S., Terenzi, G., 2001. Non-linear dynamic modelling and design procedure of FV spring-dampers for base isolation. Engineering Structures, 23, 1556–1567.

Sorace, S., Terenzi, G., Fadi, F., 2012. Shaking table and numerical seismic performance evaluation of a fluid viscous-dissipative bracing system. Earthquake Spectra, 28, 1619–1642.

Sorace, S., Terenzi, G., Mori, C., 2016. Passive energy dissipation-based retrofit strategies for R/C frame water storage tanks. Engineering Structures, 106, 385-398.

Terenzi, G., 1999. Dynamics of SDOF systems with nonlinear viscous damping. Journal of Engineering Mechanics ASCE, 125, 956–963.

Terenzi, G., 2018. Energy-based design criterion of dissipative bracing systems for seismic retrofit of framed structures. Applied Sciences 8, 268, doi:10.20944/preprints201801.0086.v1.